scientific reports

Check for updates

OPEN

Inactivation of phosphodiesterase-4B gene in rat nucleus accumbens shell by CRISPR/Cas9 or positive allosteric modulation of the protein affects the motivation to chronically self-administer nicotine

Burt M. Sharp[1✉], Qin Jiang[1], Panjun Kim[1] & Hao Chen[2]

Large scale human genome wide association studies (GWAS) have identified a growing pool of genes associated with cigarette smoking. One of the most prominent, phosphodiesterase-4B (PDE4B), has been associated with multiple smoking phenotypes. Although PDE4B modulates the half-life of neuronal cAMP, its precise role in smoking behaviors is unknown. To address this knowledge gap, we used a reverse translational approach. We inactivated *PDE4B* in bilateral medial nucleus accumbens shell (NAcs) neurons by injecting AAV containing a specific gRNA in female transgenic Cas9+ Long Evans rats. These rats then were given 23-h chronic access to nicotine intravenous self-administration (IVSA) under a schedule of increasing fixed ratios (FR). With the increased effort required at FR7, nicotine SA (i.e. active presses and drug infusions) declined significantly in controls, whereas it was maintained in the mutagenized group. A progressive ratio (PR) study also showed significantly greater cumulative nicotine infusions in the PDE4B-edited group. Hence, we hypothesized that enhanced PDE4B protein activity would reduce nicotine IVSA. A positive allosteric modulator, 2-(3-(4-chloro-3-fluorophenyl)-5-ethyl-1H-1,2,4-triazol-1-yl)-N-(3,5-dichlorobenzyl)acetamide (MR-L2), was microinfused into NAcs bilaterally at FR3 or FR5; in both cohorts, MR-L2 acutely reduced nicotine IVSA. In summary, these studies show that the activity of PDE4B regulates the capacity of NAcs to maintain nicotine IVSA in face of the cost of increasing work. This finding and the results of the PR study indicate that PDE4B affects the motivation to obtain nicotine. These reverse translational studies in rats provide insight into the motivational effects of NAcs PDE4B that advance our understanding of the smoking behaviors mapped in human GWAS.

Human genome wide association studies (GWAS) have identified a growing pool of genes associated with cigarette smoking[1,2]. A study of 1.2 million individuals in the British Biobank identified phosphodiesterase-4B (PDE4B) as one of only three genes[2] independently associated with multiple smoking phenotypes including initiation of regular smoking, age of regular smoking, amount smoked (cigarettes/day), and smoking cessation[1,2]. Recently, meta-analysis of a GWAS involving 60 ancestrally diverse cohorts, comprised of 3.4 million individuals, found seven distinct single nucleotide polymorphisms (SNPs) in an intron of phosphodiesterase-4B

---

[1]Department of Genetics, Genomics and Informatics, College of Medicine, University of Tennessee Health Science Center, Memphis, TN, USA. [2]Department of Pharmacology, Addiction Science and Toxicology, College of Medicine, University of Tennessee Health Science Center, Memphis, TN, USA. ✉email: labsharp1@gmail.com

nature portfolio

1

(PDE4B)—each associated with smoking initiation across ancestral groups[2]. As genes associated with tobacco smoking are confirmed by human GWAS, understanding the functional significance of specific genes has become increasingly important in the rational selection of novel therapeutic targets to improve the success of smoking cessation[2,3]. Reverse translational modeling of human GWAS findings in established animal models of addiction is a potent tool for understanding the behavioral function of specific genes[4].

PDE4B belongs to a multi-gene family of PDE isoenzymes that regulate cyclic nucleotide homeostasis in multiple intracellular compartments[5]. PDE4B is one of four PDE4 isoenzymes (A,B,C,D) encoded by four genes that specifically dephosphorylate cyclic AMP (cAMP), selectively limiting the half-life of cAMP-dependent signaling by signaling complexes involved in specific cellular processes[6,7]. Therefore, the PDE4B expressed in nucleus accumbens (NAc)[8], a pivotal brain region involved in the network mediating the motivation to take drugs including nicotine[9,10], is most likely a critical regulator of signaling pathways controlling the activation of medium spiny neurons (MSNs) in NAc.

The neural circuitry of NAc, largely comprised of MSNs, functions as the brain interface critically involved in the motivation for goal directed behaviors by integrating information from cortical and limbic inputs with outputs to brain regions involved in goal-directed behaviors (e.g., ventral pallidum). By regulating the half-life of cAMP associated with signaling complexes in MSNs, PDE4B affects the activity of key downstream signaling molecules including protein kinase A (PKA), dopamine and cAMP-regulated phosphoprotein (DARPP-32), and cAMP-response element binding protein (CREB)[11,12]. These signaling molecules modulate the excitability of MSNs[13–15]. Signaling in this pathway (i.e., cAMP/PKA/DARPP-32/CREB) is activated by dopamine receptors (D1R), in response to dopamine release induced by nicotine and other drugs of abuse, and inhibited by D2R; these dopamine receptor (DaR) subtypes are differentially expressed by two types of MSNs[16–18].

The effects of modulating PDE4B activity on operant intravenous self-administration (IVSA) of nicotine are unknown. Based on human GWAS that have demonstrated the association of PDE4B with human smoking behavior[1,2], we addressed the role of PDE4B in operant nicotine IVSA by using a well-established rat model of virtually unlimited chronic access to the drug[19,20]. Studies have distinguished the functions of NAc shell vs core in behavioral paradigms such as operant nicotine IVSA and reinstatement of extinguished nicotine seeking, respectively[9,10,21], and have shown that D2R MSN projecting to ventral pallidum from medial NAc shell regulate motivation for food[22]. Hence, we focused on NAc shell because of its relevance to motivated nicotine-taking in our operant model[19,20].

We sought to disrupt PDE4B gene expression in medial NAc shell (NAcs) neurons, by in vivo genome editing using virally delivered gRNA targeting all transcripts of PDE4B in transgenic rats containing CRISPR/Cas9[23]. To accomplish this and to selectively target neurons controlling motivation that project to ventral pallidum, rats received bilateral medial NAcs microinjections of adeno-associated virus (AAV) containing the PDE4B gRNA. In retrograde transport studies, we had previously shown that medial NAcs neurons project to ventral pallidum[24]. Additional experiments were designed to enhance the activity of PDE4B protein in NAc by administering a positive allosteric modulator (PAM) specific for PDE4 long isoenzymes, which contain two upstream conserved regulatory regions (i.e., UCR1 and UCR2)[7,25]. This PAM, 2-(3-(4-chloro-3-fluorophenyl)-5-ethyl-1H-1,2,4-triazol-1-yl)-N-(3,5-dichlorobenzyl)-acetamide (MR-L2), targets UCR1 and has been shown to reduce cellular cAMP levels and PKA signaling[7,25]. We found that inactivating the PDE4B gene in NAcs neurons by CRISPR/Cas9-induced mutation increased the motivation to obtain nicotine as the FR requirement increased (i.e., number of operant lever presses required to obtain a single i.v. infusion of nicotine), whereas administration of MR-L2 had the opposite effect—decreasing the motivation to obtain nicotine.

Methods

Materials, animals and breeding

Heterozygous loxP-STOP-loxP Cas9+ female outbred Long Evans rats, originally developed by Brandon K. Harvey Ph.D. at NIH[23], and provided by Dr. Aron Geurts at Medical College of Wisconsin, were used in all experiments. We maintained a breeding colony using wildtype Long Evans rats from Charles River, and genotyped (Transnetyx, Memphis, TN) to identify Cas9+ females. The following numbers of animals were included in the data analysis of each experiment: 10 rats for analysis of genome edits; 26 in studies of nicotine SA including progressive ratio (excluded: an additional 5 rats with jugular cannula occlusions); 18 received NAcs infusions of MR-L2 vs. vehicle during nicotine SA at FR3 (excluded: an additional 4 with cannula occlusions); 23 received MR-L2 vs. vehicle during nicotine SA at FR5 (excluded: an additional 7 with cannula occlusions).

2-(3-(4-Chloro-3-fluorophenyl)-5-ethyl-1H-1,2,4-triazol-1-yl)-N-(3,5-dichlorobenzyl)acetamide (MR-L2) was from Targetmol Chemicals, Wellesley Hills, MA (CAS#2374703-19-0). An MR-L2 stock solution (5.0 mM) in 100% DMSO was diluted with 20% Sulfobutylether-β-Cyclodextrin (SBE-β-CD; CAS #182410-00-0; Targetmol Chemicals Inc.) in sterile saline. All animal studies were conducted under an approved protocol in accordance with the ethical standards of the Institutional Animal Care and Use Committee (IACUC) of the University of Tennessee Health Science Center (UTHSC) and the NIH guide for the care and use of laboratory animals. Euthanasia was performed by thoracotomy under lethal isoflurane anesthesia. The methods reported herein accord with ARRIVE guidelines.

Identification of an effective gRNA complementary to rat PDE4

In consultation with Applied Biological Materials Inc., Richmond, BC, Canada, we designed three gRNAs to rat PDE4B, using their proprietary software, and generated viral vectors (10^{12} GC/ml) with the following structure: pAAV-hSyn-Kozak-iCre-P2A-mClover3-U6-gRNA. Using the one effective gRNA construct, we compared 40 nl (4×10^4 genome copy of AAV, n = 2) and 400 nl injections (4×10^5 genome copy of AAV, n = 6). We sampled from 4–5 coronal PFC tissue sections (100 μm) based on the fluorescence intensity of mClover3 in sentinel sections.

Genomic DNA was extracted from the tissue sections and amplified using PCR primers surrounding the gRNA target site (5′ primer: gacagcaaaagtcacatgcag; 3′: gaacaaatggggccttaaca). Amplification of this gDNA site was performed via Hi-Plex approach optimized by Floodlight Genomics (Knoxville, TN), followed by multiplex sequencing using a single end 150 kit on an Illumina HiSeq X (San Diego, CA). Data was analyzed by CRISPRpic[26] to identify and classify mutations. Only one gRNA, TGCATGTGAGGGGCCGATTA, effectively edited the PDE4B DNA. This gRNA is on chr5:122128512–122128531 (Rnor6.0) and chr5:117359381–117359400 (mRatBN7.2). We evaluated two additional gRNAs using the foregoing method. These gRNAs did not generate edits: GTAGGT TACGAAGGTGTCGG and CATGTAGGTTACGAAGGTGT.

Stereotaxic surgery

The same procedure was used for: (1) in vivo CRISPR/Cas9 mutagenesis of neuronal PDE4B genomic DNA in nucleus accumbens shell (NAcs); (2) implantation of NAcs guide cannulae to deliver MR-L2. To avoid the considerable day-to-day variation in nicotine SA observed in pilot studies of male LE rats, females were used throughout these studies.

Female Cas9+ LE rats, 180–200 g b.wt., were anesthetized with 2% isoflurane and microinfused (300 nl/side) with AAV or control constructs (AAV-hU6-GLuc219-gRNA-EF1α-EGFP-KASH; 3.68E+12 GC/ml; from Dr. Brandon Harvey)[23] targeted bilaterally to medial NAcs (AP 1.8; ML 1.4 or − 1.4; DV 6.7; 5°). For administration of MR-L2 during nicotine IVSA, rats were implanted with guide cannulae in medial NAcs bilaterally and affixed to the skull with screws and dental cement. Ten days later, while anesthetized, a jugular vein cannula was implanted and tunneled subcutaneously to a button affixed to an incision on the back; a spring-loaded tether was attached to deliver nicotine. All procedures and protocols were approved by the IACUC of UTHSC.

Access to virtually unlimited operant nicotine SA

Rats were individually housed in operant chambers and given access to nicotine SA (23 h/day, 7 days/week, beginning at 9AM) without food deprivation or training[19,20]. Operant chambers contained two horizontal levers; during IVSA sessions, a green cue light above each lever signaled nicotine was available. Lever presses were recorded and syringe pumps were controlled by computers, using GS3 software (Coulbourn Instruments, Allentown, PA). Nicotine IVSA began on initiation of the dark cycle (10 AM/12 h). Pressing the active lever elicited a nicotine injection (0.03 mg/kg per 50 μl/0.81 s, free base, pH 7.2–7.4). To prevent an overdose, green cue lights were extinguished and nicotine was unavailable for 7 s after each nicotine injection. Pressing the inactive lever had no programmed consequence. The final hour of the 12 h lights-on cycle (9:00–10:00 AM) was reserved for animal husbandry. Catheter patency was checked with brevital injection (0.2 ml; JHP pharmaceuticals, Rochester, MI). Rats with occluded catheters were excluded from study.

Nicotine SA under progressive ratio schedule

During a single 23 h session, rats obtained nicotine under the following schedule of increasing lever press requirements for successive injections: 4, 6, 9, 12, 15, 20, 25, 32, 40, 50, 62, 77, 95, 118, 145 etc., as derived from the exponential formula [5 exp (injection number × 0.2) − 5][27]. Breakpoints were defined as the final ratio completed during a 23 h session.

Experiment 1: Increasing fixed ratio (FR) required to obtain nicotine in rats with bilateral PDE4B mutations in medial NAcs vs. controls

Stable nicotine intake in daily 23 h sessions was achieved within 10 days of initiating nicotine IVSA at FR1 (1 active lever press triggered 1 nicotine infusion); thereafter, the FR requirement was advanced as follows: FR2, 5 days; FR3, 5 days; FR5, 7 days; FR7, 7 days. Thereafter, cardiac perfusion under lethal isoflurane was performed with 4% paraformaldehyde, then brains were removed and dehydrated in 30% sucrose for 2 days. Coronal cryostat sections (100 μm) were obtained from all rats for fluorescence microscopy (excitation, 505 nm; emission, 515 nm); sections were evaluated from all rats.

Experiment 2: Effects of bilateral NAcs infusions of MR-L2 vs. vehicle control during operant nicotine IVSA at increasing FR requirements

The FR schedule was: FR1, 10 days; FR2, 5 days, FR3, 5 days, FR5, 9 days. MR-L2 or vehicle was administered on day 6 of FR3 in one group and on day 8 of FR5 in a separate group. During the final hour of lights-on, microinfusion needles were inserted into guide cannulae while rats were briefly anesthetized with 2% isoflurane; anesthesia ceased, MR-L2 (300 nl; 2 × 10⁻⁴ M; 1:20, DMSO in 20% SBE-β-CD) or vehicle (1:20, DMSO in 20% SBE-β-CD) was microinfused (25 nl/min over 12 min) into NAcs, and needles were removed 5 min later. Rats returned to home operant chambers 20 min later, the dark phase of the light cycle began, and nicotine was available. Following the experiment, brains were removed from rats treated with lethal isoflurane + thoracotomy. Brains were flash frozen, maintained at − 20 °C, and cryosectioned (50 μm) to locate guide cannulae.

Data analysis and statistics

Active lever presses and nicotine infusions at FR7 and during a PR (progressive ratio) study were compared in AAV experimental and control groups. For studies of MR-L2, similar parameters were compared during FR3 or FR5 in independent experiments. Cumulative active presses and infusions were divided into consecutive 3-h bins on the day that MR-L2 or vehicle was injected in each experiment. These data were expressed as a percentage of the mean value for the corresponding time bins recorded during the 3 preceding days.

Nicotine infusion data were normally distributed. Active and inactive presses were log transformed to obtain normal distributions for statistical analyses. Levene test for homogeneity of variance was not significant for the number of injections (p = 0.33) or log-transformed lever presses (p = 0.29). Data were analyzed by repeated measures 2-way ANOVA, using R package, with either day of lever press or nicotine infusion designated as a within-subject factors and treatment designated as a between-subject factor. Tukey HSD test was used for post hoc testing. PR data were compared between treatment groups by t-test. Time bin data were analyzed using repeated measures ANOVA, followed by pre-planned contrasts between treatments for each time bin using the emmeans package. Data were expressed as mean ± SEM. Statistical significance was assigned at $p < 0.05$.
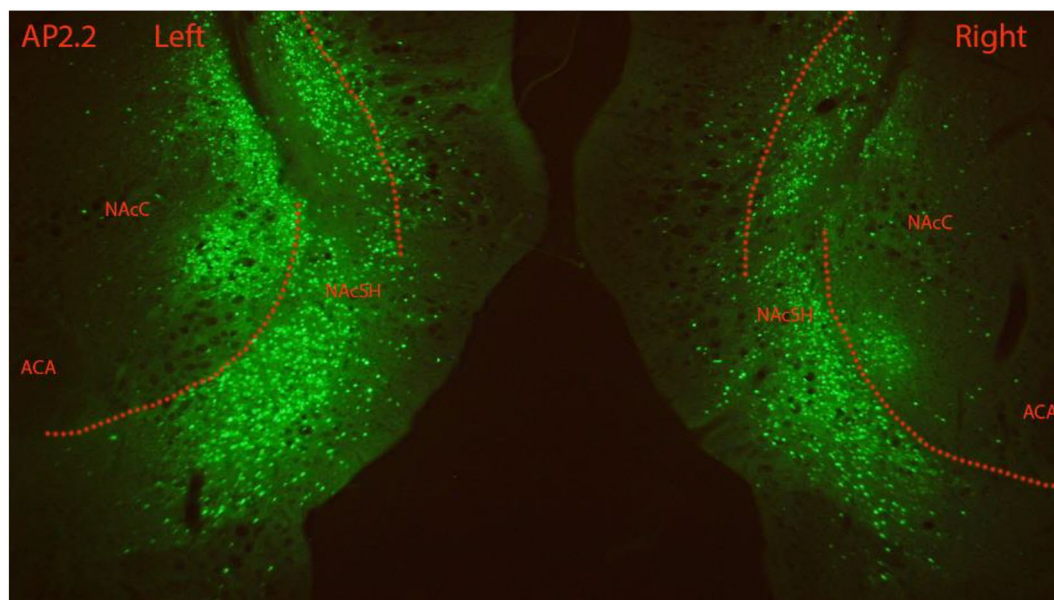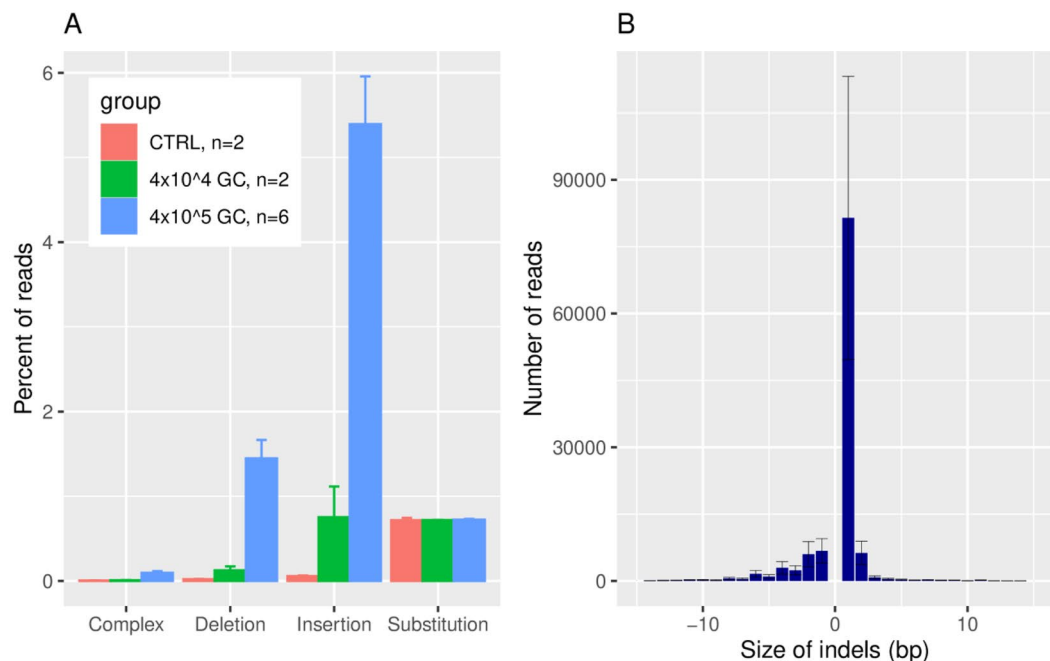

Figure 1. Detection of genome editing in prefrontal cortex and photomicrographs of mClover fluorescence in NAcs. To characterize the genome editing, prefrontal cortex (PFC) was microinjected in vivo with pAAV8-hSyn-Kozak-iCre-P2A-mClover3-U6-gRNA or control construct and tissue was obtained 10 days later (panels **A**,). Expression of mClover3 (panel **C**) was detected in NAcs 45 days post-injection of pAAV8 construct, following completion of a trial of nicotine SA through FR7. (**A**) The gRNA targeting exon 9 of PDE4B induced edits in PFC genomic DNA in a dose-dependent manner. The percent of reads that contain edits is in line with expectations for a heterogeneous tissue. Complex edits contain both insertion and deletion. *GC* genome copy. (**B**). The size of indels range from − 81 to 79 bp. The vast majority (95 ± 0.5%) of these edits will produce frame shifts, leading to loss of protein function. C. mClover fluorescence demonstrates strong expression of viral vector in NAcs neurons.

Results

Using the CRISPR/Cas9 technology targeted to neurons by neuron-specific expression of iCre and, therefore, Cas9, a gRNA specific for rat PDE4B exon 9, common to all PDE4B transcripts, generated several types of edits (Fig. 1) detected in heterogeneous tissue dissected from the medial NAcs after AAV injection. We selectively
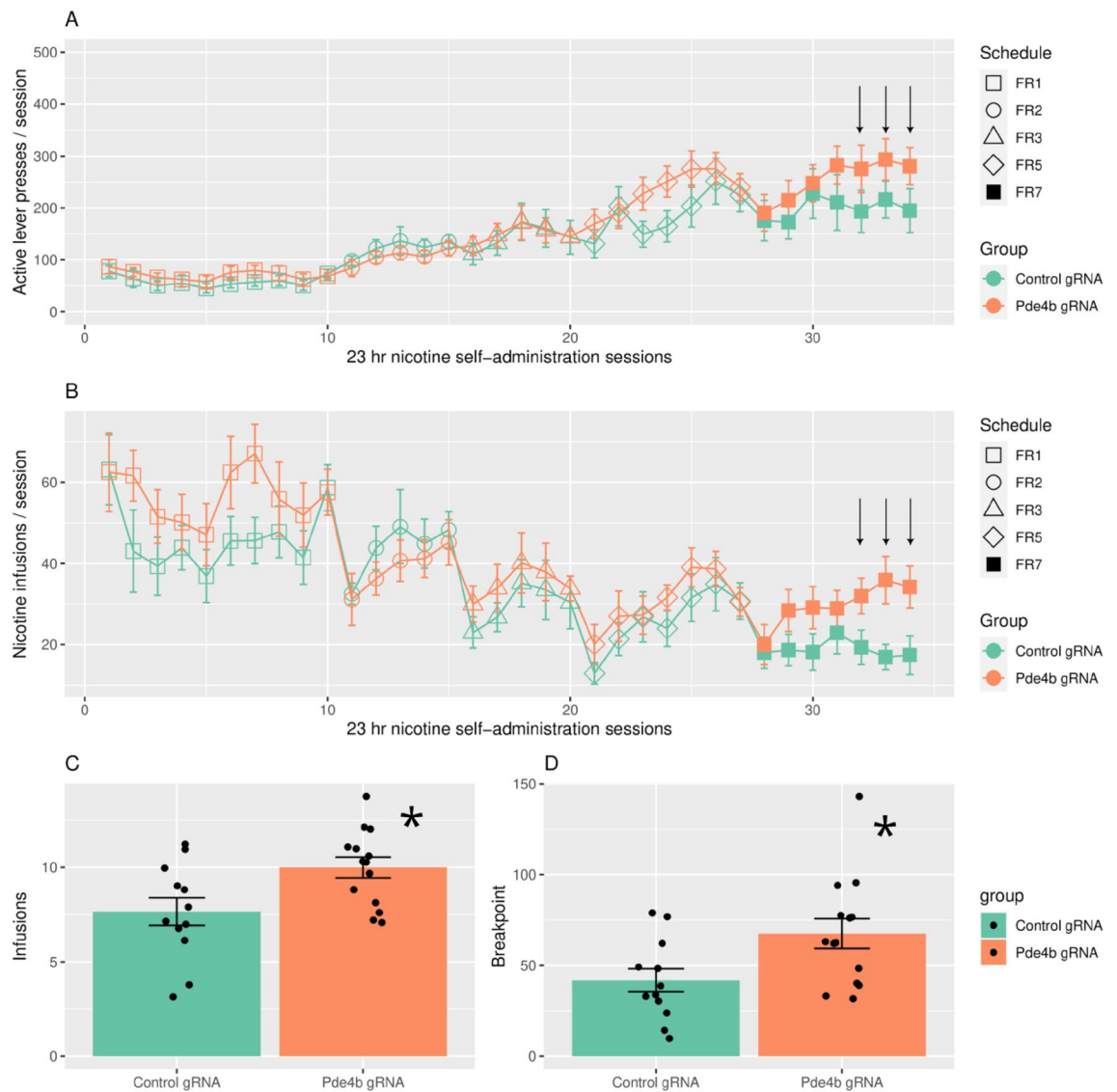

Figure 2. Operant nicotine SA under an increasing fixed ratio (FR) schedule and progressive ratio (PR) test in rats treated with AAV-Pde4b-gRNA or control (CNT) constructs. Rats had access to nicotine SA every day for 23 h/day in operant chambers equipped with active and inactive levers. Daily active lever presses (**A**) and nicotine injections (**B**) are shown according to FR schedule for both treatment groups. Repeated measures ANOVA found a main effect of day ($p < 2e-16$), as well as FR schedule ($p < 2e-16$), on the number of active lever presses, but not of treatment [control gRNA (CNT, n = 12) vs Pde4b gRNA (EXPerimental, n = 14); $p = 0.22$]. Treatment × schedule was significant ($p = 5.4e-5$). Treatment only had an effect on active presses at FR7 (Tukey, $p = 0.006$), but not at FR5 ($p = 0.60$) or other FRs. The average daily active presses at FR7: EXP, 347 ± 23.6; CNT, 229.9 ± 18.0. Similarly, for nicotine infusions, the main effects of day ($p < 2e-16$) and FR schedule ($p = 8.8e-15$) were significant. While the effect of treatment ($p = 0.16$) on nicotine infusion was not significant, treatment × FR schedule was ($F_{4,781} = 4.6$, $p = 0.001$). Treatment only had an effect on nicotine infusions at FR7 (Tukey, $p = 0.02$), but not at FR5 ($p = 0.92$) or other FRs. The average daily nicotine infusions were: EXP, 30.0 ± 1.9; CNT, 18.8 ± 1.6. The effects of FR5 vs FR7 on infusions and active presses were compared, using the day 5–7 group (marked by arrows) from each FR (infusion: treatment, $p = 0.03$; days 5–7, $p = 0.007$; treatment × days 5–7, $p = 0.01$; Tukey, CNT FR7 < CNT FR5, $p = 0.019$ and CNT FR7 < EXP FR7, $p = 0.0003$. Active presses: treatment, $p = 0.04$; days 5–7, $p = 0.99$; treatment × days 5–7, $p = 0.007$; Tukey, CNT FR7 < EXP FR7, $p = 0.00045$.). In the PR test, conducted a day after completion of nicotine SA at FR7, the cumulative infusions (**C**) obtained by the two treatment groups were: EXP = 10.0 ± 0.5 (mean ± SE; n = 14) vs. CNT = 7.7 ± 0.7 (n = 12) (*$p < 0.02$; unpaired T-test, 2-tailed). In addition, the breakpoint (**D**) achieved by the EXP group (67.6 ± 8.2 active presses) was significantly greater than CNT (41.8 ± 6.4 active presses; * $p < 0.02$).

introduced loss of function edits into the PDE4B gene of NAcs neurons in Loxp-STOP-Loxp-CRISPR/Cas9 knockin rats[23]. Neuronal specificity was achieved by injecting an AAV vector containing an hSyn promoter, which drives the expression of iCre, and a gRNA targeting exon 9 of PDE4B, present only in PDE4B transcripts (i.e., pAAV8-hSyn-Kozak-iCre-P2A-mClover3-U6-gRNA). The efficacy of this construct was evaluated by extracting DNA from heterogeneous tissue dissected from the prefrontal cortex 10 days after AAV injection. The genomic sequence flanking the gRNA target site was amplified using PCR and sequenced on an Illumina NovaSeq instrument. This tissue is approximately two thirds glial and one third neuronal[28]. However, only a relatively small subset of cells from the neurons infected by the AAV would yield edited sequences. Considering the diffusion volume of the AAV infusate and the injection site, we estimated that only 25–35% of the neurons in the sampled tissue punch could be transfected by the AAV.

Since one third of the tissue was neuronal and 25–35% of all neurons could be transfected, approximately 8–12% of all cells were actually targeted for editing. In line with this expectation, approximately 6.9 ± 1.9 percent of the sequenced reads contained edits in rats that received the PDE4B gRNA injection (Fig. 1A). By far, the most frequent type of edit was a 1 bp insertion, followed by 1 bp deletion (Fig. 1B). In total, edits ranged in size from -81 to 79 bp. Each of these types of edits, i.e., insertions, deletions and complex changes in PDE4B, were approximately 95, 75 and 20-fold, respectively, more common in tissue treated in vivo with PDE4B-gRNA compared to control (AAV-hU6-GLuc219-gRNA-EF1α-EGFP-KASH)[23]. The fold-change depended on the dose of AAV injected. Insertions, for example, were reduced from 95-fold to 13-fold greater than control by decreasing the dose tenfold. The vast majority ($95 \pm 0.5\%$) of these mutations are known to produce frameshifts, which result in the loss of protein function.

A representative photomicrograph of mClover fluorescence from one rat brain at AP 2.2 is shown in Fig. 1C. Abundant fluorescence, similar to that detected in all rats 45 days after injection of the AAV PDE4B-gRNA construct and completion of a trial of nicotine SA through FR7, is predominantly in nuclei within the NAc shell of this representative sample. Hence, Cas9-dependent mutagenesis, targeted to PDE4B by the PDE4B-gRNA, is localized to neurons largely in the medial NAc shell.

Experiment 1

Figure 2 shows active lever presses (top 2 panels) and nicotine infusions by day as FR increased from FR1 to FR7. Repeated measures ANOVA found a significant main effect of day ($F_{33,814} = 22.78$, $p < 2e{-}16$) as well as FR schedule ($F_{4,810} = 55.0$, $p < 2e{-}16$), on the number of active lever presses, but not of treatment [control gRNA (CNT, n = 12) vs Pde4b gRNA (EXPerimental, n = 14); $F_{1,20} = 1.62$, $p = 0.22$]. However, treatment × schedule had a significant interaction ($F_{4,781} = 6.3$, $p = 5.4e{-}5$). Posthoc Tukey test found that treatment only had a significant effect on active presses at FR7 ($p = 0.006$), but not at FR5 ($p = 0.60$) or other FRs. The average daily active presses at FR7 were: EXP, 347 ± 23.6; CNT, 229.9 ± 18.0. Similarly, for nicotine infusions, the main effects of day ($F_{33,814} = 11.0$, $p < 2e{-}16$) and FR schedule ($F_{4,100} = 26.0$, $p = 8.8e{-}15$) were highly significant. While the effect of treatment ($F_{1,20} = 2.2$, $p = 0.16$) on nicotine infusion was not significant, there was a significant interaction between treatment and FR schedule ($F_{4,781} = 4.6$, $p = 0.001$). Posthoc Tukey tests found that treatment only had a significant effect on nicotine infusions at FR7 (Tukey, $p = 0.02$), but not at FR5 ($p = 0.92$) or other FRs. The average daily nicotine infusions were: EXP, 30.0 ± 1.9; CNT, 18.8 ± 1.6.

We further analyzed the effects of treatment on nicotine infusions and active presses during each of the seven days of FR7. Infusions and active presses were only affected on days 5–7 of FR7 (nicotine infusions: treatment, $F_{1,22} = 4.16$, $p = 0.05$; day, $F_{1,22} = 4.16$, $p = 0.05$; treatment × day, $F_{6,142} = 1.72$, $p = 0.12$; contrasts, day 5, $t = -1.85$, $p = 0.07$; day 6, $t = -2.76$, $p = 0.008$; day 7, $t = -2.44$, $p = 0.018$. Active presses: treatment, $F_{1,22} = 2.9$, $P = 0.1$; day, $F_{6,142} = 1.69$, $p = 0.13$; treatment × day, $F_{6,142} = 2.3$, $p = 0.04$; contrasts, day 5, $t = -2.27$, $p = 0.03$; day 6, $t = -1.95$, $p = 0.05$; day 7, $t = -2.32$, $p = 0.03$). We then compared the effects of FR5 vs FR7 on infusions and active presses, using the day 5–7 group from each FR (infusions: treatment, $F_{1,24} = 5.36$, $p = 0.03$; days 5–7, $F_{1,99} = 7.55$, $p = 0.007$; treatment × days 5–7, $F_{1,99} = 6.937.46$, $p = 0.01$; Tukey, CNT FR7 < CNT FR5, $p = 0.019$ and CNT FR7 < EXP (i.e., PDE4B) FR7, $p = 0.0003$. Active presses: treatment, $F_{1,24} = 4.6$, $p = 0.04$; days 5–7, $F_{1,99} = 0.000$, $p = 0.99$; treatment

Figure 3. Operant nicotine SA under an increasing fixed ratio (FR) schedule in rats treated on day 6 with MR-L2 (EXP) or vehicle (SBE) at FR3. Active and inactive presses and infusions are shown for MR-L2 (**A** MR-L2 2×10^{-4} M, 300 nl/side; n = 9) and vehicle control (**B** DMSO-SBE; n = 9) groups. Repeated measures ANOVA on the number of active presses during the day of injection and three days prior found an effect of the experimental stage (i.e. prior vs post injection, $p = 0.01$) and interaction between stage and experimental group (MR-L2 vs SBE, $p = 0.01$). Comparing days 3–6, MR-L2, but not SBE, significantly reduced active presses on day 6 (MR-L2, $p = 7.14e{-}5$; SBE, $p = 0.96$). Similarly, an effect of experimental stage ($p = 0.01$) and an interaction ($p = 0.01$) between stage and experimental group were found on the number of nicotine infusions, which were reduced by MR-L2 on day 6 (MR-L2, $p = 6.67e{-}5$; SBE, $p = 0.99$). Inactive presses from both treatment groups (i.e., panels **A,B**) were analyzed by ANOVA: treatment, $p = 0.576$; stage, $p = 0.02$; interaction, $p = 0.05$. EXP, stage: $p = 0.002$; SBE, stage: $p = 0.75$. Total active presses elicited or infusions were binned in time intervals 0–3, 3–6, 6–9, and 9–12 h after administration of MR-L2 into NAcs bilaterally. These data were normalized by the average value for the corresponding time bins recorded on days 3–5. (**C**) Treatment affected active presses ($p = 0.03$), as did time bin ($p = 6.2e{-}05$). Pre-planned contrasts found the effect of treatment was only significant between 3 nad 6 h (t.ratio = -2.32, $p = 0.02$). (**D**) Similarly, the main effect of treatment on nicotine infusion was significant ($p = 0.01$), whereas the effect of time bin was not ($p = 0.14$). Pre-planned contrasts found the effect of treatment was only significant between 3 and 6 h (t.ratio = -2.25, $p = 0.03$). A schematic (**E**) showing the NAcs locations of all injection needle tips used to administer MR-L2 to rats on day 6 of the 7-day FR3 schedule. The brain section was adapted from the rat brain atlas of Paxinos and Watson[30].
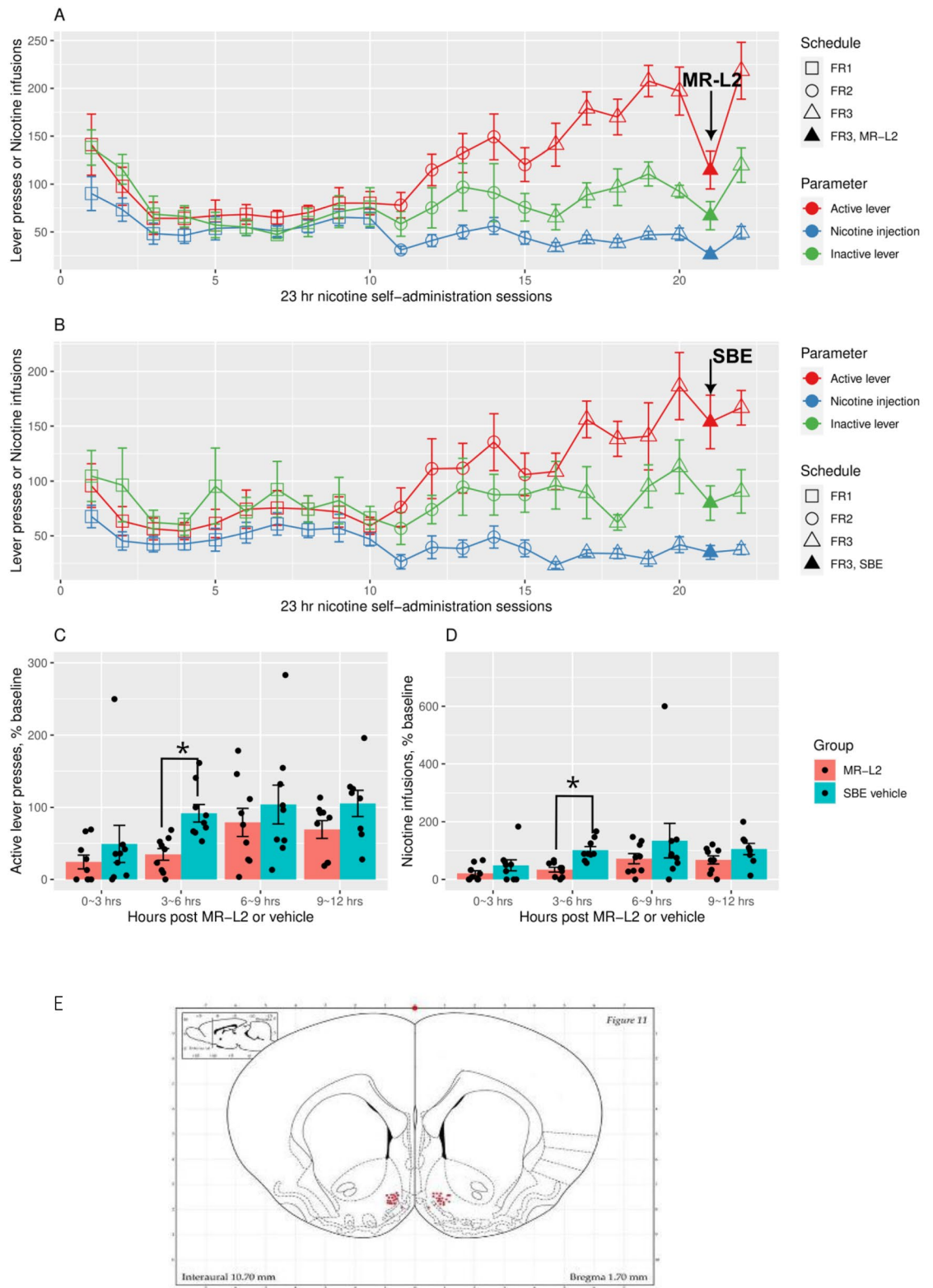
× days 5–7, F1,99, 7.46, p = 0.007; Tukey, CNT FR7 < EXP (i.e., PDE4B) FR7, p = 0.00045.). Therefore, in the CNT group, nicotine infusions were significantly reduced during days 5–7 at FR7 compared to FR5. In contrast, infusions did not decline at FR7 vs FR5 in the EXP group. On days 5–7 at FR7, both infusions and active presses were less in CNT compared to EXP.

Since inactive presses and locomotion measured using breaks of infrared beams have been shown to covary during nicotine-enhanced operant responding[29], we used inactive presses as a valid surrogate measure of nicotine-stimulated locomotion. In our study, inactive presses were affected by the escalating reinforcement schedule ($F_{4,100}$ = 4.27, p = 0.003) and by day ($F_{33,814}$ = 2.78, p = 5.35e−07), but not by treatment ($F_{1,20}$ = 0.71, p = 0.41). An interaction between treatment and escalating FRs was found ($F_{4,781}$ = 3.67, p = 0.006), but unlike for active levers, there was no treatment effect on inactive presses at FR7 (Tukey, p = 0.99).

Lastly, a progressive ratio (PR) test was conducted the day after the completion of nicotine IVSA at FR7. Figure 2 (lower panels: a,b) shows the cumulative infusions and breakpoints achieved in the two treatment groups: infusions, EXP = 10.0 ± 0.5 vs. CNT = 7.7 ± 0.7 (t = − 2.56, Df = 24 p = 0.018); breakpoints, EXP = 67.6 ± 8.2 active presses vs CNT = 41.8 ± 6.4 (t = − 2.48, Df = 24 p = 0.02). In summary, region-specific editing of PDE4B in medial NAcs sustained lever pressing to self-administer i.v. nicotine despite the high FR requirement (i.e. FR7), whereas active presses and nicotine infusions declined in the CNT group. This difference is reinforced by the significant difference in infusions and breakpoints achieved during the PR test—an index of motivation to obtain nicotine.
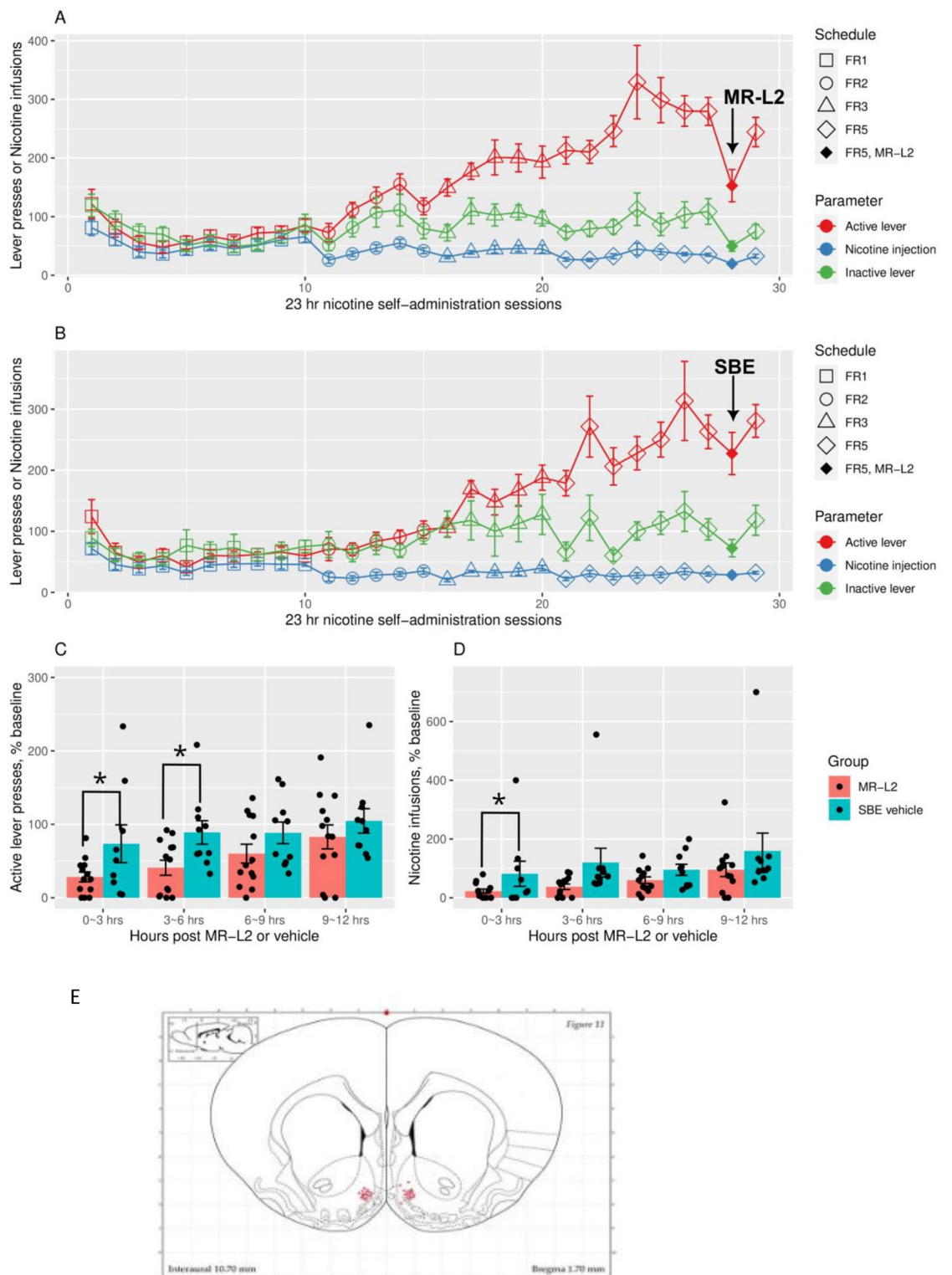
Experiment 2

Rats with bilateral NAcs guide cannula implants self-administered nicotine under a schedule of increasing FR. Figure 3E is a schematic showing the NAcs positions of the injection needle tips used to administer MR-L2 (2×10^{-4} M, 300 nl/side) on day 6 of the 7-day FR3 schedule. Almost all injection tips were tightly localized to medial NAcs.

Figure 3A,B shows the effect of MR-L2 on active presses and infusions at FR3 in EXP (panel A; n = 9) and vehicle control (i.e., received DMSO-SBE; n = 9) groups. Repeated measures ANOVA on number of active presses during the day of injection and three days prior found a significant effect of the experimental stage (i.e. prior vs post injection, $F_{1,48}$ = 6.5, p = 0.01) and significant interaction ($F_{1,48}$ = 6.9, p = 0.01) between stage and experimental group (MR-L2 vs vehicle). MR-L2 significantly reduced active lever presses on day 6, compared to three prior days ($F_{1,24}$ = 22.91, p = 7.14e−5), but the effect of vehicle (SBE) was not significant ($F_{1,24}$ = 0.002, p = 0.96). Similarly, repeated measures ANOVA on the number of nicotine infusions during the day of injection and three days prior found a significant effect of the experimental stage ($F_{1,48}$ = 6.9, p = 0.01) and significant interaction ($F_{1,48}$ = 7.0, p = 0.01) between stage and experimental group. MR-L2 significantly reduced active lever presses on day 6, compared to three prior days ($F_{1,24}$ = 23.2, p = 6.67e−5), but the effect of SBE was not significant ($F_{1,24}$ = 0.001, p = 0.99). Repeated measures ANOVA on number of inactive presses in panels A and B during the day of injection and three days prior: treatment, $F_{1,16}$ = 0.326, p = 0.576; stage, $F_{1,48}$ = 6.02, p = 0.02; interaction, $F_{1,48}$ = 3.89, p = 0.05. ANOVA on inactive in panel A: EXP, stage: $F_{1,24}$ = 11.56, p = 0.002 and ANOVA on inactive in panel B: SBE, stage: $F_{1,24}$ = 0.10, p = 0.75. Therefore, MR-L2 significantly reduced inactive presses, whereas administration of SBE in the control group had no effect.

In Fig. 3C,D, we further analyzed the effects of MR-L2 by generating time bins containing all active presses elicited or infusions obtained within time intervals 0–3, 3–6, 6–9, and 9–12 h after administration of MR-L2. These data were normalized by the average value for each time bin recorded on days 3–5. Figure 3C,D shows that the greatest effects of MR-L2 (EXP) vs. SBE on active presses and infusions occurred between 3 and 6 h after dosing. The main effect of treatment on active presses was significant ($F_{1,16}$ = 5.6, p = 0.03), as was that of the time bin ($F_{3,64}$ = 8.7, p = 6.2e−05). Pre-planned contrasts found the effect of treatment was only significant between 3 and 6 h (t.ratio = − 2.32, p = 0.02). Similarly, the main effect of treatment on nicotine infusion was significant ($F_{1,16}$ = 7.5, p = 0.01), while the effect of time bin was not ($F_{4,48}$ = 1.9, p = 0.14). Pre-planned contrasts found the effect of treatment was only significant between 3 and 6 h (t.ratio = − 2.25, p = 0.03).

Figure 4E is a schematic showing the NAcs positions of the injection needle tips used to administer MR-L2 (2×10^{-4} M, 300 nl/side) on day 8 of the 9-day FR5 schedule. The effects of MR-L2 on active presses and nicotine infusions at FR5 in EXP (n = 13) and vehicle control (i.e., DMSO-SBE; n = 10) groups are shown in Fig. 4A,B. Repeated measures ANOVA on the number of active presses during the day of stereotaxic injection and three

Figure 4. Operant nicotine SA under an increasing fixed ratio (FR) schedule in rats treated on day 8 with MR-L2 (EXP) or vehicle (SBE) at FR5. Active and inactive presses and infusions are shown for MR-L2 (**A** MR-L2 2×10^{-4} M, 300 nl/side; n = 13) and control (**B** DMSO-SBE; n = 10) groups. Comparing experimental stage (i.e., days 5–7 vs injection day 8), MR-L2, but not SBE, significantly reduced active presses on day 8 in MR-L2: p = 1.55e−05; treatment × stage, p = 0.005 (repeated measures ANOVA). Similarly, nicotine infusions were significantly reduced by MR-L2 on day 8: day, p = 3.69e-05; treatment × stage, p = 0.004. Inactive presses in panels A and B during the experimental stage (i.e., day of injection and 3 days prior): treatment, p = 0.44; stage, p = 3.72e−07; interaction, p = 0.25. ANOVA on inactive in panel (**A**) MR-L2, stage: p = 0.0001; ANOVA on inactive in panel (**B**) SBE, stage: p = 0.0006. Therefore, both SBE and MR-L2 significantly reduced inactive presses. Panels (**C,D**) show total active presses elicited or infusions binned by time intervals 0–3, 3–6, 6–9, and 9–12 h after administration of MR-L2 into NAcs bilaterally. These data were normalized by the average value for the corresponding time bins recorded on days 5–7. Effects on active presses were found: treatment, (p = 0.03); time bin, (p = 1.45e−05). Pre-planned contrasts: treatment was only significant at 0–3 h (t.ratio = − 2.23, p = 0.03) and 3–6 h (t.ratio = − 2.60, p = 0.01). Effects on nicotine infusion: treatment, (p = 0.02); time bin (p = 0.54). Pre-planned contrasts: treatment was only significant at 0–3 h (t.ratio = 2.6, p = 0.01). A schematic[30] showing the NAcs locations of all injection needle tips used to administer MR-L2 to rats on day 8 of the 9-day FR5 schedule.

days prior found an effect of the experimental stage (i.e. prior 3 days vs day of stereotaxic injection; $F_{1,63} = 21.9$, p = 1.55e−05) and an interaction ($F_{1,63} = 8.4$, p = 0.005) between experimental stage and treatment group (MR-L2 vs SBE). Similarly for nicotine infusions, the effect of the experimental stage was significant ($F_{1,63} = 19.7$, p = 3.69e−05) and an interaction between stage and treatment group was found ($F_{1,63} = 9.09$, p = 0.004).

Repeated measures ANOVA on number of inactive presses in panels A and B during the day of injection and three days prior: treatment, $F_{1,21} = 0.62$, p = 0.44; stage, $F_{1,63} = 32.24$, p = 3.72e−07; interaction, $F_{1,63} = 1.34$, p = 0.25. ANOVA on inactive in panel A: EXP, stage: $F_{1,36} = 18.87$, p = 0.0001 and ANOVA on inactive in panel B: SBE: stage: $F_{1,27} = 15.2$, p = 0.0006. Therefore, both SBE and MR-L2 significantly reduced inactive presses at FR5. The inconsistent effect of SBE on inactive presses at FR3 vs FR5 strongly suggests that the reduction in active presses by MR-L2 at both FR3 and FR5 is independent from effects on inactive presses. The reduction in inactive presses is probably related to variable effects of the injection procedure including anesthesia.

Figure 4C,D shows the time bins for active presses and nicotine infusions obtained after administration of MR-L2 at FR5. The main effect of treatment on active presses was significant ($F_{1,16} = 5.5$, p = 0.03), as was that of the time bin ($F_{3,48} = 10.9$, p = 1.45e−05). Pre-planned contrasts found the effect of treatment was only significant between 0–3 h (t.ratio = − 2.23, p = 0.03) and 3–6 h (t.ratio = − 2.60, p = 0.01). Similarly, the main effect of treatment on nicotine infusion was statistically significant ($F_{1,21} = 6.3$, p = 0.02), while the effect of time bin was not ($F_{3,63} = 0.72$, p = 0.54). Pre-planned contrasts found the effect of treatment was only significant between 0 and 3 h (t.ratio = 2.6, p = 0.01).

Discussion

Although human GWAS have implicated PDE4B in multiple stages of smoking behavior[1,2], the mechanism(s) underlying these effects are unknown. We hypothesized that reducing the function of PDE4B in NAcs neurons by CRISPR/Cas9 gene inactivation and enhancing the catabolic activity of the protein using MR-L2, a positive allosteric modulator, would provide insight into the role of PDE4B in nicotine SA under a schedule of increasing FR. Indeed, selective modulation of PDE4B by administration of the gRNA or MR-L2 into medial NAcs demonstrated significant and opposite effects on the maintenance of nicotine IVSA in face of increasing FR requirements. Editing PDE4B by inducing selective deletions and insertions in an exon specific for PDE4B maintained nicotine IVSA at high FR (i.e., FR7) compared to the declining IVSA observed in controls. Conversely, positive allosteric modulation of PDE4B rapidly reduced nicotine SA at FR3 and FR5; these FRs were otherwise well tolerated in controls.

These observations were made in rats that received microinfusions of an AAV construct into NAcs bilaterally—a construct designed to specifically edit PDE4B only in neurons. We tested our hypothesis in the NAcs because of its critical role in operant nicotine SA[9,31] and the relatively high concentration of PDE4B identified in this region[8]. NAc is the brain interface that integrates mesocorticolimbic inputs, which transmit cognitive, emotive and reward-related information to NAc MSN. Monosynaptic inputs from regions such as frontal cortex, hippocampus and basolateral/basomedial amygdala[32], activate MSNs via glutamatergic projections. Additionally, nicotine-induced dopamine release from the ventral tegmental area to MSN modulates the activation of MSN[33]. The NAc circuitry generates MSN outputs to regions such as ventral pallidum, which engage the brain circuitry involved in goal directed behaviors[34,35].

The high behavioral costs necessary to obtain rewards in certain operant paradigms are surmounted by increasing NAc neuronal activity[36]. In high-cost trials, subsets of MSN fire prior to the initiation of behavioral responding and remain active until the reward is obtained, whereas the duration of responding is shorter when the cost is less[37]. The costs of these predictably large responses are encoded by differences in phasic dopamine signaling to MSN[38]. Dynamic changes in moment-to-moment dopamine release are critical to these cost-related decisions[39,40] involved in motivated behavior to obtain conditioned rewards. Based on the results of PDE4B editing, we hypothesize that the high cost of obtaining nicotine reward at FR7 is not met by increased MSN activity driven by enhanced dopamine release unless dopamine signaling is further amplified by molecular changes in the neuronal landscape, such as those induced by reducing the function of PDE4B in neurons.

PDE4B interacts with compartmentalized signaling complexes and modulates dopamine signaling by regulating the half-life of cAMP synthesized following D1R activation[5,40]. Additionally, glutamatergic signaling to MSN AMPA receptors is modulated by D1R/cAMP/PKA[41–43]. The duration and level of cAMP signaling determines the activity of downstream signaling moieties such as PKA, DARPP-32, PP1a and CREB[11,12], which are involved in regulating the excitation of MSN[13,15] and in regulation of the transcriptional landscape[44–46]. Hence, PDE4B sits at a critical juncture—impacting both the acute and chronic activation of MSN.

The acute effects of modulating PDE4B activity and, thereby, MSN excitation are exemplified by the experiments with MR-L2. We observed the effects of this compound in rats self-administering nicotine at FR3 by 3 h after infusion into NAcs (the administration protocol, which tended to reduce nicotine SA just after delivery of the drug, obviated detecting the effect of MR-L2 earlier), and the effects waned by 6 h. Since positive allosteric modulation of PDE4B attenuates cAMP signaling, we would expect it to reduce nicotine and dopamine-dependent excitation of MSN[25]. Indeed, in two separate experiments, MR-L2 reduced active lever presses and nicotine intake at both FR3 and FR5.

Conversely, chronic down-regulation of PDE4B protein, due to disruption of gene expression by induction of deletions and insertions in a coding region, resulted in the maintenance of nicotine IVSA (i.e., active presses and nicotine intake) despite high FR demand—which reduced IVSA in controls. We did not directly measure PDE4B protein, which is a limitation of this study. Reliably detecting reduced expression of PDE4B protein would be very challenging when only a small fraction of NAc neurons are edited. Notwithstanding this limitation, we would expect chronic downregulation to have more complex effects on MSN function than acute administration of a drug such as MR-L2. cAMP signaling would be tonically enhanced, thus increasing nicotine

and dopamine-dependent excitation of MSN. Additionally, resetting the transcriptional landscape and the downstream expression of neuronal proteins in multiple pathways would likely produce a myriad of changes in MSN function and in behavior that remain to be delineated. For example, in vivo transfection of constitutively active CREB has been shown to amplify the excitability of MSN[13].

The DaR subtypes (i.e. D1R and D2R) differentially expressed by two types of NAc MSNs[16–18] have opposite effects on cAMP synthesis[47]. Activation of D1R induces adenylate cyclase to synthesize cAMP, whereas D2R inhibits this enzyme[47]. Therefore, increased PDE4B activity would diminish D1R-dependent cAMP signaling and the activation of D1R-MSN; conversely, increased PDE4B activity would most likely amplify the inhibitory effect of dopamine on MSN that express D2R. Hence, PDE4B modulates both the activation and inhibition of MSN, depending in large part on the expression of D1R vs. D2R[16,17].

The effects of reducing the expression of PDE4B by CRISPR/Cas9 gene editing and enhancing the catabolic activity of the protein using MR-L2 depend on the subtype of MSN: a knock-down of the PDE4B gene would enhance D1R-dependent signaling and activation of D1R-MSN, whereas it would diminish the inhibitory effect of D2R signaling and reduce the inhibition of D2R-MSN by dopamine. Conversely, MR-L2 would be expected to reduce D1R-dependent signaling and increase D2R signaling. The relative role of each DaR-MSN subtype in determining the behavioral outcomes observed in this study are unknown. Both subtypes of NAc MSN appear to be involved in reward and aversion[48–50], depending in part on the duration of stimulation[49]. Moreover, the motivational effects of activating a specific subtype of DaR-MSN (i.e. D2R) depend on the phase of the motivated behavior (i.e. conditioned cue vs reward consumption)[51].

Nicotine is known to stimulate locomotor activity with increasing effects on repeated exposure[52]. These locomotor effects might contribute to the reward-enhancing effects of nicotine on operant responding[53], which if affected by the inactivation of PDE4B would potentially confound the interpretation of our results. Since inactive presses and beam breaks have been shown to covary during nicotine-enhanced operant responding[29], inactive presses are a valid surrogate measure of nicotine-stimulated locomotion. Our results show that nicotine intake at escalating FR did not affect inactive lever presses within either treatment group (i.e., PDE4B edited vs. control) nor was there a difference between groups. Therefore, in our behavioral paradigm of virtually unlimited access to nicotine SA, nicotine did not increase inactive presses within treatment groups, nor did it affect the level of inactive presses between groups. The effects of editing and inactivating PDE4B on sustained nicotine SA at escalating FR cannot be attributed to locomotor enhancement by nicotine.

In summary, PDE4B plays a pivotal role in determining the NAcs motivational response to conditioned nicotine reinforcement. Reduced PDE4B activity, induced by CRISPR/Cas9 frameshift-induced gene inactivation, maintains the motivation to take nicotine as the cost of work increases, whereas increased PDE4B activity impairs the motivation to take the drug. Since NAc neuronal responses to goal directed behavior are heterogenous, depending on factors such as the specific neurons sampled, the operant paradigm, and the phase of the motivated behavior[37,38,51], the observations made in the present study may depend in part on the area of NAcs (i.e. dorsomedial) affected by CRISPR/Cas9 and MR-L2. Nonetheless, these reverse translational studies provide novel insights into the role of NAcs PDE4B in operant nicotine IVSA at increasing FR workload that contribute to understanding the heretofore unexplained GWAS associations between PDE4B and multiple stages of human smoking.

Data availability

Data sets generated or analyzed in this study are available from the corresponding author on reasonable request.

References

1. Liu, M. *et al.* Association studies of up to 12 million individuals yield new insights into the genetic etiology of tobacco and alcohol use. *Nat. Genet.* **51**, 237–244 (2019).
2. Saunders, G. R. B. *et al.* Genetic diversity fuels gene discovery for tobacco and alcohol use. *Nature* https://doi.org/10.1038/s41586-022-05477-4 (2022).
3. Zhu, S.-H., Lee, M., Zhuang, Y.-L., Gamst, A. & Wolfson, T. Interventions to increase smoking cessation at the population level: How much progress has been made in the last two decades?. *Tob Control.* **21**, 110–118 (2012).
4. Venniro, M., Banks, M. L., Heilig, M., Epstein, D. H. & Shaham, Y. Improving translation of animal models of addiction and relapse by reverse translation. *Nat. Rev. Neurosci.* **21**, 625–643 (2020).
5. Francis, S. H., Blount, M. A. & Corbin, J. D. Mammalian cyclic nucleotide phosphodiesterases: Molecular mechanisms and physiological functions. *Physiol. Rev.* **91**, 651–690 (2011).
6. Conti, M. *et al.* Cyclic AMP-specific PDE4 phosphodiesterases as critical components of cyclic AMP signaling. *J. Biol. Chem.* **278**, 5493–5496 (2003).
7. Houslay, M. D. Underpinning compartmentalised cAMP signalling through targeted cAMP breakdown. *Trends Biochem. Sci.* **35**, 91–100 (2010).
8. Polesskaya, O. O., Smith, R. F. & Fryxell, K. J. Chronic nicotine doses down-regulate PDE4 isoforms that are targets of antidepressants in adolescent female rats. *Biol. Psychiatry* **61**, 56–64 (2007).
9. Scofield, M. D. *et al.* The nucleus accumbens: Mechanisms of addiction across drug classes reflect the importance of glutamate homeostasis. *Pharmacol. Rev.* **68**, 816–871 (2016).
10. Salgado, S. & Kaplitt, M. G. The nucleus accumbens: A comprehensive review. *Stereotact. Funct. Neurosurg.* **93**, 75–93 (2015).
11. Svenningsson, P., Nairn, A. C. & Greengard, P. DARPP-32 mediates the actions of multiple drugs of abuse. *AAPS J.* **7**, E353–E360 (2005).
12. Campbell, S. L., van Groen, T., Kadish, I., Smoot, L. H. M. & Bolger, G. B. Altered phosphorylation, electrophysiology, and behavior on attenuation of PDE4B action in hippocampus. *BMC Neurosci.* **18**, 77 (2017).
13. Dong, Y. *et al.* CREB modulates excitability of nucleus accumbens neurons. *Nat. Neurosci.* **9**, 475–477 (2006).

11

14. Onn, S.-P., Fienberg, A. A. & Grace, A. A. Dopamine modulation of membrane excitability in striatal spiny neurons is altered in DARPP-32 knockout mice. *J. Pharmacol. Exp. Ther.* **306**, 870–879 (2003).
15. Perez, M. F., White, F. J. & Hu, X.-T. Dopamine D(2) receptor modulation of K(+) channel activity regulates excitability of nucleus accumbens neurons at different membrane potentials. *J. Neurophysiol.* **96**, 2217–2228 (2006).
16. Nishi, A., Snyder, G. L. & Greengard, P. Bidirectional regulation of DARPP-32 phosphorylation by dopamine. *J. Neurosci.* **17**, 8147–8155 (1997).
17. Yan, Z., Feng, J., Fienberg, A. A. & Greengard, P. D(2) dopamine receptors induce mitogen-activated protein kinase and cAMP response element-binding protein phosphorylation in neurons. *Proc. Natl. Acad. Sci. USA* **96**, 11607–11612 (1999).
18. Hamada, M. *et al.* Nicotine regulates DARPP-32 (dopamine- and cAMP-regulated phosphoprotein of 32 kDa) phosphorylation at multiple sites in neostriatal neurons. *J. Pharmacol. Exp. Ther.* **315**, 872–878 (2005).
19. Valentine, J. D., Hokanson, J. S., Matta, S. G. & Sharp, B. M. Self-administration in rats allowed unlimited access to nicotine. *Psychopharmacology* **133**, 300–304 (1997).
20. Yu, G. & Sharp, B. M. Basolateral amygdala and ventral hippocampus in stress-induced amplification of nicotine self-administration during reacquisition in rat. *Psychopharmacology* **232**, 2741–2749 (2015).
21. D'Souza, M. S. & Markou, A. Differential role of N-methyl-D-aspartate receptor-mediated glutamate transmission in the nucleus accumbens shell and core in nicotine seeking in rats. *Eur. J. Neurosci.* **39**, 1314–1322 (2014).
22. Sellings, L. H. L., Baharnouri, G., McQuade, L. E. & Clarke, P. B. S. Rewarding and aversive effects of nicotine are segregated within the nucleus accumbens. *Eur. J. Neurosci.* **28**, 342–352 (2008).
23. Bäck, S. *et al.* Neuron-specific genome modification in the adult rat brain using CRISPR-Cas9 transgenic rats. *Neuron* **102**, 105-119.e8 (2019).
24. Chen, H. *et al.* Genome-wide gene expression profiling of nucleus accumbens neurons projecting to ventral pallidum using both microarray and transcriptome sequencing. *Front. Neurosci.* **5**, 98 (2011).
25. Omar, F. *et al.* Small-molecule allosteric activators of PDE4 long form cyclic AMP phosphodiesterases. *Proc. Natl. Acad. Sci. USA* **116**, 13320–13329 (2019).
26. Lee, H., Chang, H. Y., Cho, S. W. & Ji, H. P. CRISPRpic: Fast and precise analysis for CRISPR-induced mutations via prefixed index counting. *NAR Genom. Bioinform.* **2**, 2 (2020).
27. Arnold, J. M. & Roberts, D. C. A critique of fixed and progressive ratio schedules used to examine the neural substrates of drug reinforcement. *Pharmacol. Biochem. Behav.* **57**, 441–447 (1997).
28. Bandeira, F., Lent, R. & Herculano-Houzel, S. Changing numbers of neuronal and non-neuronal cells underlie postnatal brain growth in the rat. *Proc. Natl. Acad. Sci. USA* **106**, 14108–14113 (2009).
29. Barret, S. T. & Bevins, R. A. Nicotine enhances operant responding for qualitatively distinct reinforcers under maintenance and extinction conditions. *Pharmacol. Biochem. Behav.* **114–115**, 9–15 (2013).
30. Paxinos, G. Paxinos and Watson's the rat brain in stereotaxic coordinates. 1997.
31. Corrigall, W. A., Franklin, K. B., Coen, K. M. & Clarke, P. B. The mesolimbic dopaminergic system is implicated in the reinforcing effects of nicotine. *Psychopharmacology* **107**, 285–289 (1992).
32. Li, Z. *et al.* Cell-type-specific afferent innervation of the nucleus accumbens core and shell. *Front. Neuroanat.* **12**, 84 (2018).
33. Liu, C., Goel, P. & Kaeser, P. S. Spatial and temporal scales of dopamine transmission. *Nat. Rev. Neurosci.* **22**, 345–358 (2021).
34. Leung, B. K. & Balleine, B. W. The ventral striato-pallidal pathway mediates the effect of predictive learning on choice between goal-directed actions. *J. Neurosci.* **33**, 13848–13860 (2013).
35. Fujimoto, A. *et al.* Signaling incentive and drive in the primate ventral pallidum for motivational control of goal-directed action. *J. Neurosci.* **39**, 1793–1804 (2019).
36. Hauber, W. & Sommer, S. Prefrontostriatal circuitry regulates effort-related decision making. *Cereb. Cortex* **19**, 2240–2247 (2009).
37. Day, J. J., Jones, J. L. & Carelli, R. M. Nucleus accumbens neurons encode predicted and ongoing reward costs in rats. *Eur. J. Neurosci.* **33**, 308–321 (2011).
38. Day, J. J., Jones, J. L., Wightman, R. M. & Carelli, R. M. Phasic nucleus accumbens dopamine release encodes effort- and delay-related costs. *Biol. Psychiatry* **68**, 306–309 (2010).
39. Salamone, J. D. & Correa, M. Motivational views of reinforcement: Implications for understanding the behavioral functions of nucleus accumbens dopamine. *Behav. Brain Res.* **137**, 3–25 (2002).
40. Hamid, A. A. *et al.* Mesolimbic dopamine signals the value of work. *Nat. Neurosci.* **19**, 117–126 (2016).
41. Chao, S. Z., Ariano, M. A., Peterson, D. A. & Wolf, M. E. D1 dopamine receptor stimulation increases GluR1 surface expression in nucleus accumbens neurons. *J. Neurochem.* **83**, 704–712 (2002).
42. Anderson, S. M. *et al.* CaMKII: A biochemical bridge linking accumbens dopamine and glutamate systems in cocaine seeking. *Nat. Neurosci.* **11**, 344–353 (2008).
43. Sun, X., Milovanovic, M., Zhao, Y. & Wolf, M. E. Acute and chronic dopamine receptor stimulation modulates AMPA receptor trafficking in nucleus accumbens neurons cocultured with prefrontal cortex neurons. *J. Neurosci.* **28**, 4216–4230 (2008).
44. Vialou, V. *et al.* Serum response factor and cAMP response element binding protein are both required for cocaine induction of ΔFosB. *J. Neurosci.* **32**, 7577–7584 (2012).
45. Kronman, H. *et al.* Biology and bias in cell type-specific RNAseq of nucleus accumbens medium spiny neurons. *Sci. Rep.* **9**, 8350 (2019).
46. Lardner, C. K. *et al.* Gene-targeted, CREB-mediated induction of ΔFosB controls distinct downstream transcriptional patterns within D1 and D2 medium spiny neurons. *Biol. Psychiatry* **90**, 540–549 (2021).
47. Beaulieu, J.-M. & Gainetdinov, R. R. The physiology, signaling, and pharmacology of dopamine receptors. *Pharmacol. Rev.* **63**, 182–217 (2011).
48. Bin Saifullah, M. A. *et al.* Cell type-specific activation of mitogen-activated protein kinase in D1 receptor-expressing neurons of the nucleus accumbens potentiates stimulus-reward learning in mice. *Sci. Rep.* **8**, 14413 (2018).
49. Soares-Cunha, C. *et al.* Nucleus accumbens medium spiny neurons subtypes signal both reward and aversion. *Mol. Psychiatry* **25**, 3241–3255 (2020).
50. Yao, Y. *et al.* Projections from D2 neurons in different subregions of nucleus accumbens shell to ventral pallidum play distinct roles in reward and aversion. *Neurosci. Bull.* **37**, 623–640 (2021).
51. Soares-Cunha, C. *et al.* Distinct role of nucleus accumbens D2-MSN projections to ventral pallidum in different phases of motivated behavior. *Cell Rep.* **38**, 110380 (2022).
52. Bevins, R. A. & Besheer, J. Individual differences in rat locomotor activity are diminished by nicotine through stimulation of central nicotinic acetylcholine receptors. *Physiol. Behav.* **72**, 237–244 (2001).
53. Frenk, H. *et al.* Reward potentiation or behavioral activation? A comment on Donny. *Psychopharmacology* **171**, 472–473 (2004).

Acknowledgements

Author contributions

B.S.: conceptualized and designed the experiments; analyzed data; wrote and revised the manuscript. Q.J.: conducted surgeries and behavioral experiments. P.K.: assisted with analysis of DNA data. H.C.: co-designed gRNAs and AAV constructs and contributed to the design of experiments; analyzed data; edited graphics and manuscript.

Competing interests

The authors declare no competing interests.

Additional information

Correspondence and requests for materials should be addressed to B.M.S.

Reprints and permissions information is available at www.nature.com/reprints.

Publisher's note Springer Nature remains neutral with regard to jurisdictional claims in published maps and institutional affiliations.